Bioprocess Engineering 9 (1993) 1–12

Bioprocess Engineering

Mixing-models applied to industrial batch bioreactors

B. Mayr, Graz, Austria **P. Horvat,** Zagreb, Croatia **E. Nagy** Veszprém, Hungary and **A. Moser,** Graz, Austria

Abstract. Mixing models for bioreactors on the basis of the tanks-in-series concept are presented and a suitable parameter-estimation method is introduced. The Monte-Carlo-optimization procedure with the inhomogeneity-curve included in the objective function is used. Results of the parameter optimization procedure are given for stirred-tank-bioreactors equipped with one and three Rushton turbines under aerated conditions. The model designed for the stirred-tank with three Rushton turbines is capable to describe the mixing properties, while in case of the stirred-tank with one Rushton turbine the simulated radial circulation time does not correlate with the measured one.

List of symbols

$a_{00} \cdots a_{XY}$	-	coefficients in Eq. (9)
d_i	m	stirrer diameter
D	m	tank diameter
E	-	relative error
F_{AX}	m^3/s	axial liquid flow rate
F_G	m^3/s	aeration flow rate
F_{RAD}	m^3/s	radial liquid flow rate
g	m/s^2	acceleration of gravity
h_l	m	height of fluid in the tank
$i_s(t)$	-	simulated inhomogeneity-curve
$i_m(t)$	-	measured inhomogeneity-curve
k	-	number of sensors
n	1/s	stirrer revolutions
N	-	number of tanks in the tanks-of-series-cascade
p	-	number of measured time intervalls
t	s	time
$t_{c,AX}$	s	axial circulation time
$t_{c,RAD}$	s	radial circulation time
T_i	°C	temperature of sensors
T_∞	°C	temperature at the end of the experiment
T_0	°C	temperature before pulse injection
V_{tot}	m^3	total liquid volume
V_C	m^3	liquid volume of circulation cascade, additional index specifications describe the cascade elements (Figs. 1 and 2)
V_M	m^3	liquid volume of well mixed stirrer compartment
w_0	m/s	superficial gas velocity
X, Y	-	exponents in eq. (9)
ρ	kg/m^3	density
η	Pas	dynamic viscosity
ν	m^2/s	kinematic viscosity
τ	s	time constant (time for 63,2% of T_∞) of the signal

Dimensionless numbers

$$Fr_S = n\sqrt{d_i/g} \qquad \text{stirrer Froude number}$$

$$Fr_A = \frac{w_0}{\sqrt{g \cdot h_l}} = \frac{F_G}{V_{tot}} \cdot \sqrt{\frac{h_l}{g}} \qquad \text{aeration Froude number}$$

1 Introduction

During the last two decades several stirred tank models have been suggested, mainly based on the concept of a micromixed volume in vicinity of the stirrer and macromixed recirculation loops [1–23, 29]. Only a few articles describe mixing in industrial bioreactors measured with a multiple sensor system. Khang and Levenspiel [9] used the conductivity method, while in the other works the heat pulse technique was applied [20, 25, 26, 29]. Usally the pulse was either poured to the liquid surface [20, 23] or injected in the stirrer region by means of a special system [9, 26]. The experimental conditions recorded with a one-sensor system might lead to significant inaccuracies in the parameter identification process [23], since the mixing behaviour of the whole tank is defined by only one signal describing one "point" in the vessel, i.e. a small volume around the sensor [24]. A recent study proved that mean deviations in the mixing times measured at different points in the tank reach 60% related to the inhomogeneity time valid for the whole tank [26].

So far a study of the model parameters on the basis of extensive and exact measurements in industrial pilot-plant scale bioreactors is missing, but only such a work provides the ability to make safe scale-up predictions from laboratory to industrial scale [28], since these models can easily be coupled with equations defining microbial kinetics, oxygen and heat transfer [11, 13, 21, 23].

The aim of this study was to develop physical mixing models and a parameter-estimation procedure by using the inhomogeneity-curve [26] and the Monte-Carlo-optimization-method. The results are presented for stirred-tank bioreactors equipped with one or three Rushton

turbines, with liquid volumes of 1.2 m^3 and 2.5 m^3, respectively. 62 experiments with a mixture of glycerol and tapwater as test medium are included in this study, covering a wide operational range of the tested fermentors.

2 Material and methods

2.1 Fermentors

Bioreactors with technical features given in Table 1 were examined. All bioreactors are supplied with 4 baffles, geometrical details are given elsewhere [26].

2.2 Measurements

The temperature pulse method [18, 20, 25, 26] was used to investigate the flow properties. Six PT-100 sensors were positioned in the bioreactors [26] and their responses to the temperature pulse was recorded by means of an electronic interface connected to a personal computer.

The experimental conditions are given in Table 2. All combinations of stirrer rotations with aeration rates were tested. The temperature was kept in the range between 22°C to 26°C. The viscosity of the test medium was chosen to be comparable to the viscosity of antibiotic fermentation broths.

2.3 The physical mixing-models

In this work a tanks-in-series model approach is utilized, for the description of mixing properties in tanks equipped with either one or three stirrers.

2.3.1 Model for the stirred tank bioreactor with 1 Rushton turbine (STR-1)

The model used was suggested by Singh et al. in 1986 [12]. Looking at the macroscopic flow pattern of the reactor with one Rushton turbine (Fig. 1a) two main regions can be distinguished:

a) About 70% of the stirring energy is dissipated in the immediate vincinity of the turbine [30–37,45]. Due to the high local energy input in the stirrer region the fluid around the turbine is assumed to be perfectly mixed and therefore represented in the model (Fig. 1b) with an ideally mixed compartment (V_M).

b) In the remaining volume of the tank (V_c) the flow recirculates in two main regions, i.e. above and below the stirrer section. Away from the stirrer the turbulent intensity decreases rapidly, but additional mixing is achieved at high aeration rates. These regions are combined in the

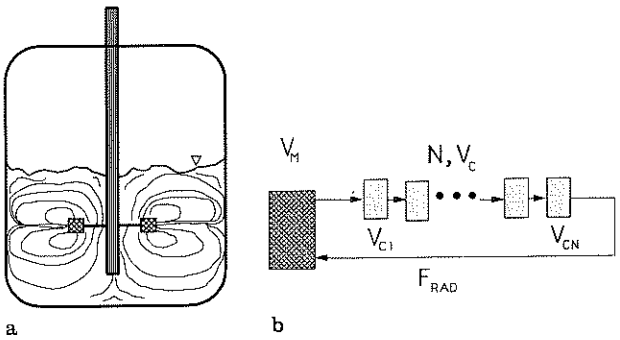

Fig. 1. Macroscopic flow pattern (a) and physical mixing model (b) for the STR-1 stirred tank bioreactor

Table 1. Technical features of the bioreactors

Synonym –	Tank volume m^3	Stirrer –	Turbine diameter m	max. Power kW	Tank diameter m	h_l/D –	Liquid volume m^3
STR-1	3.2	1 Rushton	0.51	26	1.18	1.1	1.2
STR-3	3.2	3 Rushton	0.51	26	1.18	2.3	2.5

Table 2. Experimental conditions

Fermentor –	Stirrer revolutions rps	Aeration rate m^3/h	Power input kW	Medium –	Density kg/m^3	Viscosity Pa-s
STR-1	1; 1.67; 2.5; 3.3; 4.17	0; 40; 70; 100; 150; 200	0.12–18.5	Glycerol-water	1218.1	0.18
STR-3	1; 1.67; 2.5; 3.3; 4.17	0; 40; 70; 100; 150; 200	0.26 - 26	Glycerol-water	1218.1	0.18

model and are represented by one cascade of ideally mixed and equally sized tanks (Fig. 1b).

The solution (Eq. (1)) of the system of differential equations is describing the response function in all compartments of the model illustrated in Fig. 1b. The pulse of tracer is represented by a vector of inhomogeneities $\delta(t)$. The matrix A_1 is given in Eq. (2) :

$$\frac{d}{dt}\begin{bmatrix} T_M \\ T_{C,1} \\ \cdot \\ \cdot \\ \cdot \\ T_{C,N} \end{bmatrix} = A_1 \begin{bmatrix} T_M \\ T_{C,1} \\ \cdot \\ \cdot \\ \cdot \\ T_{C,N} \end{bmatrix} + \begin{bmatrix} \delta(t) \\ 0 \\ \cdot \\ \cdot \\ \cdot \\ 0 \end{bmatrix} \tag{1}$$

$$A_1 = \begin{array}{c} \\ M \\ C1 \\ \vdots \\ CN \end{array} \begin{array}{c} \begin{array}{cccccc} T_M & T_{C1} & 0 & \cdots & 0 & T_{CN} \end{array} \\ \begin{bmatrix} -\frac{F_{RAD}}{V_M} & 0 & \cdots & 0 & \frac{F_{RAD}}{V_M} \\ \frac{F_{RAD}}{V_C} & -\frac{F_{RAD}}{V_C} & 0 & \cdots & 0 \\ \vdots & \vdots & \vdots & \vdots & \vdots \\ \frac{F_{RAD}}{V_C} & 0 & \cdots & 0 & -\frac{F_{RAD}}{V_C} \end{bmatrix} \end{array} \tag{2}$$

Three adjustable parameters are included in the mathematical model:

a) The ratio of ideally mixed volume to total liquid volume (V_M/V_{tot}) ,
b) the radial circulation time ($t_{c,RAD}$) , defined according to Eq. (3) and
c) the number of ideally mixed tanks (N) in the cascade

$$t_{c,RAD} = \frac{V_{tot}}{F_{RAD}} \tag{3}$$

The positions of the three response functions of the model are defined as follows:

a) The first one is situated in the ideally mixed stirrer volume (V_M) simulating the arithmetic mean of the measured responses at the sensors 3 and 4 [26].
b) The second one is situated in the volume after one third of the tank-in-series (V_C) (e.g. in case of $N = 6$ the second tank) related to the mean of the measured reponses at the sensors 2 and 5 [26].
c) The third one is situated in the volume after two thirds of the tank-in-series (V_C) (e.g. in case of $N = 6$ the fourth tank), related to the mean of the measured responses at the sensors 1 and 6 [26].

2.3.2 Model for the stirred tank with 3 Rushton turbines (STR-3)

Fig. 2b shows the model which is an extended version of a model proposed by Singh et al. [12]. On basis of the macroscopic flow pattern (Fig. 2a) the bioreactor can be seperated into three regions, each of them is related to one stirrer section and is characterized by an ideally mixed compartment around the stirrer and two macromixers, i.e. a cascade of tanks-in-series, describing the recirculation flow. This model is actually an extension of the STR-1 model with only one additional adjustable parameter, the axial circulation time ($t_{c,AX}$) , therefore the statements made for the STR-1 are also valid here. The radial and the axial circulation times are defined according to Eqs. (4, 5) respectively:

$$t_{c,RAD} = \frac{V_{tot}}{3*F_{RAD}} , \tag{4}$$

$$t_{c,AX} = \frac{V_{tot}}{F_{AX}} . \tag{5}$$

The position of the axial exchange flow between the top region (V_{M1}, V_{C1}, V_{C2}) of the vessel and the middle region (V_{M2}, V_{C3}, V_{C4}) was assigned to the middle volume element in the adjoining cascades (i.e. $V_{C2,J}$ and $V_{C3,J}$), the interchange between the middle and the lower region is located in the middle volume of the adjoining cascades (i.e. $V_{C4,J}$ and $V_{C5,J}$).

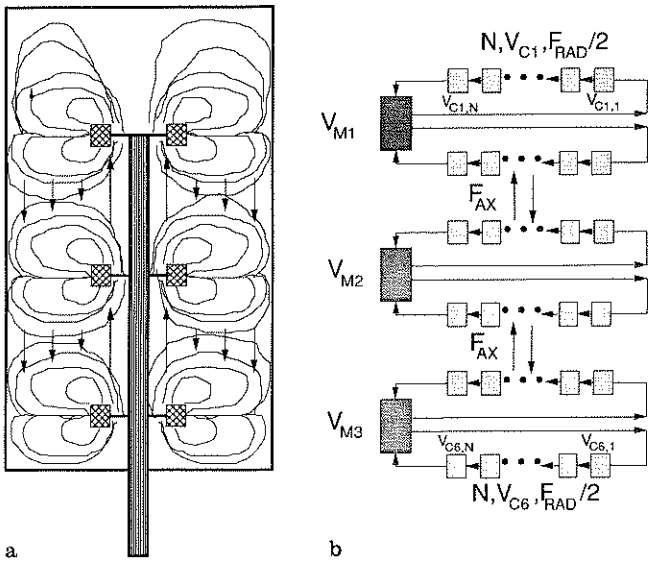

Fig. 2. Macroscopic flow pattern (a) and physical mixing model (b) for the STR-3 stirred tank bioreactor $V_{M1} = V_{M2} = V_{M3} = V_M/3$, $V_{Cij} = V_C/(6N)$

The set of differential equations is presented in Eq. (6):

$$\frac{d}{dt}\begin{bmatrix} T_{M1} \\ T_{C1,1} \\ \vdots \\ T_{C1,N} \\ T_{C2,1} \\ \vdots \\ T_{C2,N} \\ T_{M2} \\ T_{C3,1} \\ \vdots \\ T_{C3,N} \\ T_{C4,1} \\ \vdots \\ T_{C4,N} \\ T_{M3} \\ T_{C5,1} \\ \vdots \\ T_{C5,N} \\ T_{C6,1} \\ \vdots \\ T_{C6,N} \end{bmatrix} = A_2 \begin{bmatrix} T_{M1} \\ T_{C1,1} \\ \vdots \\ T_{C1,N} \\ T_{C2,1} \\ \vdots \\ T_{C2,N} \\ T_{M2} \\ T_{C3,1} \\ \vdots \\ T_{C3,N} \\ T_{C4,1} \\ \vdots \\ T_{C4,N} \\ T_{M3} \\ T_{C5,1} \\ \vdots \\ T_{C5,N} \\ T_{C6,1} \\ \vdots \\ T_{C6,N} \end{bmatrix} + \begin{bmatrix} 0 \\ \vdots \\ \delta(t)_{TOP} \\ \vdots \\ \vdots \\ \vdots \\ \vdots \\ \vdots \\ \vdots \\ \vdots \\ \delta(t)_{CENTRAL} \\ \vdots \\ \vdots \\ \vdots \\ \vdots \\ \vdots \\ \vdots \\ \vdots \end{bmatrix} \quad (6)$$

The pulse injection in the model was assigned to the last element of the fourth cascade ($V_{C4,N}$) before reentering the middle ideally mixed volume in case of a central pulse input and to element ($V_{C1,N}$) for a pulse application to the surface. These two possibilities are indicated in Eq. (6) by two elements in the vector of inhomogeneities $\delta(t)$. The matrix A_2 is given in Eq. (7).

(Equation 7 see next page)

The positions of the five response functions of the model are defined as follows:

The response functions one to three are positioned in the ideally mixed stirrer volumes (V_{M1}, V_{M2}, V_{M3}), the measured sensor response 1 is assigned to V_{M1}, the mean of the experimental curves recorded at positions 3 and 4 is related to V_{M2}, sensor 6 to V_{M3}.

The fourth response function is positioned between top and middle region of the physical model and simulates the temperature response at sensor 2.

The fifth response function is positioned in the transient part between the middle and lower region of the bioreactor and is related to sensor 5.

Two modifications of this model were tested. The first one is the original model presented by Singh et al. [12]. In the second modification an attempt to incorporate the gas-holdup was made. The gas replaces a certain amount of liquid in the fermentor, so that an increase of liquid level is observed. This expansion was simulated in the model as an increase of the liquid volume in the top circulation loop (V_{C1}), while the liquid volume of all other regions is being reduced.

2.4 Mathematical methods

2.4.1 Numerical Solution of the differential equation system

The system is a set of linear first-order ordinary differential equations coupled with a term describing the pulse. In case of a Dirac-pulse-function the integration can be done either analytically by means of Laplace-transformation and subsequent inverse transformation [3] or by applying a numerical method. Since the presented models are almost always described by numerous equations, the inverse Laplace-transformation becomes clumsy and therefore the Runge-Kutta-Fehlberg-algorithm (RKF) [38] is used. It utilizes the local truncation error of order five to estimate the local error in a Runge-Kutta-method of order four [39]. This error estimate also controls the step width of integration.

2.4.2 Non linear optimization of mixed integer and real parameters

Generally coupled linear differential equation systems with mixed integer and real adjustable parameters show more than one optimum. Therefore an algorithm capable of finding the global optimum is needed. A further complication is that one of the model parameters, i.e. N, is an integer. Virtually all optimization methods for non-linear problems are iterative. They begin with an initial guess for the fitting parameters and make sucessive refinements. As the parameters approach their optimal values the subsequent refinements become smaller.

In this work four methods were tested, a Gauss-Newton-method [40], a Collocation-method using the Davidon-Fletcher-Powell (DFP) update formula [41], a hybrid method applying the DFP update as a Levenberg type modifier for the Gauss Newton algorithm [40] and a Monte-Carlo method [42]. Finally the Monte-Carlo-optimization method was selected.

2.4.3 Parameter estimation with optimization

The identification process consists basically of three steps, which will be discussed in the following sections.

$$
\mathbf{A}_2 = \begin{array}{c} \\ M1 \\ C1,1 \\ \vdots \\ C1,N \\ C2,1 \\ \vdots \\ C2,J \\ \vdots \\ C2,N \\ M2 \\ C3,1 \\ \vdots \\ C3,J \\ \vdots \\ C3,N \\ C4,1 \\ \vdots \\ C6,N \end{array}
\begin{array}{c}
\begin{array}{ccccccccccccccccccc}
T_{M1} & & T_{C1,1} & \cdots & T_{C1,N} & T_{C2,1} & \cdots & T_{C2,J} & \cdots & T_{C2,N} & T_{M2} & T_{C3,1} & \cdots & T_{C3,J} & \cdots & T_{C3,N} & T_{C4,1} & \cdots & T_{C6,N}
\end{array} \\
\begin{bmatrix}
-\frac{3}{V_M}F_{RAD} & 0 & \cdots & +\frac{1.5}{V_M}F_{RAD} & 0 & \cdots & 0 & \cdots & +\frac{1.5}{V_M}F_{RAD} & 0 & 0 & \cdots & 0 & \cdots & 0 & 0 & \cdots & 0 \\
+\frac{3N}{V_C}F_{RAD} & -\frac{3N}{V_C}F_{RAD} & \cdots & 0 & 0 & \cdots & 0 & \cdots & 0 & 0 & 0 & \cdots & 0 & \cdots & 0 & 0 & \cdots & 0 \\
\vdots & \vdots & & \vdots & \vdots & & \vdots & & \vdots & \vdots & \vdots & & \vdots & & \vdots & \vdots & & \vdots \\
0 & 0 & \cdots & -\frac{3N}{V_C}F_{RAD} & 0 & \cdots & 0 & \cdots & 0 & 0 & 0 & \cdots & 0 & \cdots & 0 & 0 & \cdots & 0 \\
+\frac{3N}{V_C}F_{RAD} & 0 & \cdots & 0 & -\frac{3N}{V_C}F_{RAD} & \cdots & 0 & \cdots & 0 & 0 & 0 & \cdots & 0 & \cdots & 0 & 0 & \cdots & 0 \\
\vdots & \vdots & & \vdots & \vdots & & \vdots & & \vdots & \vdots & \vdots & & \vdots & & \vdots & \vdots & & \vdots \\
0 & 0 & \cdots & 0 & 0 & \cdots & -\frac{6N}{V_C}\left(\frac{F_{RAD}}{2}-F_{AX}\right) & \cdots & 0 & 0 & 0 & \cdots & +\frac{6N}{V_C}F_{AX} & \cdots & 0 & 0 & \cdots & 0 \\
\vdots & \vdots & & \vdots & \vdots & & \vdots & & \vdots & \vdots & \vdots & & \vdots & & \vdots & \vdots & & \vdots \\
0 & 0 & \cdots & 0 & 0 & \cdots & 0 & \cdots & -\frac{3N}{V_C}F_{RAD} & 0 & 0 & \cdots & 0 & \cdots & 0 & 0 & \cdots & 0 \\
0 & 0 & \cdots & 0 & 0 & \cdots & 0 & \cdots & 0 & -\frac{3}{V_M}F_{RAD} & 0 & \cdots & 0 & \cdots & +\frac{1.5}{V_M}F_{RAD} & 0 & \cdots & 0 \\
0 & 0 & \cdots & 0 & 0 & \cdots & 0 & \cdots & 0 & +\frac{3N}{V_C}F_{RAD} & -\frac{3N}{V_C}F_{RAD} & \cdots & 0 & \cdots & 0 & 0 & \cdots & 0 \\
\vdots & \vdots & & \vdots & \vdots & & \vdots & & \vdots & \vdots & \vdots & & \vdots & & \vdots & \vdots & & \vdots \\
0 & 0 & \cdots & 0 & 0 & \cdots & +\frac{6N}{V_C}F_{AX} & \cdots & 0 & 0 & 0 & \cdots & -\frac{6N}{V_C}\left(\frac{F_{RAD}}{2}+F_{AX}\right) & \cdots & 0 & 0 & \cdots & 0 \\
\vdots & \vdots & & \vdots & \vdots & & \vdots & & \vdots & \vdots & \vdots & & \vdots & & \vdots & \vdots & & \vdots \\
0 & 0 & \cdots & 0 & 0 & \cdots & 0 & \cdots & 0 & 0 & 0 & \cdots & 0 & \cdots & -\frac{3N}{V_C}F_{RAD} & 0 & \cdots & 0 \\
0 & 0 & \cdots & 0 & 0 & \cdots & 0 & \cdots & 0 & +\frac{3N}{V_C}F_{RAD} & 0 & \cdots & 0 & \cdots & 0 & -\frac{3N}{V_C}F_{RAD} & \cdots & 0 \\
\vdots & \vdots & & \vdots & \vdots & & \vdots & & \vdots & \vdots & \vdots & & \vdots & & \vdots & \vdots & & \vdots \\
0 & 0 & \cdots & 0 & 0 & \cdots & 0 & \cdots & 0 & 0 & 0 & \cdots & 0 & \cdots & 0 & 0 & \cdots & -\frac{3N}{V_C}F_{RAD}
\end{bmatrix}
\end{array}
$$

2.4.3.1 Calculation of significant criteria of the experiment. The following criteria were used to describe the experimental curves:

a) Homogeneity-times [26] for inhomogeneity-degrees of 0.1 and 0.2 in order to quantify the last section of the mixing experiment.

b) The maximum value of the inhomogeneity curve [26], which gives a first guess on the dispersion behaviour at the beginning.

c) The time constants of the individual signals are the time intervals between pulse injection time and the time the signal reaches 63.2% of the end temperature T_∞. The differences in the time constants give good approximations for the flow transit time ($\Delta\tau$) between the locations of the sensors.

2.4.3.2 Selecting initial values for model parameters. The starting point for the optimization process is of major importance, since several local optima might occur. In order to detect the global optimum the initial point must be in a suitable region. To achieve this requirement a test of the model was carried out and the results for the mentioned criteria for about 1000 simulations with different parameter combinations were stored in a database. The measured results are compared with the stored simulated values and the parameter combination with smallest absolute deviation is selected as initial combination.

2.4.3.3 Optimization of the model parameters. With the initial combination of the model parameters the Monte-Carlo-procedure is launched. Boundaries for all adjustable parameters must be selected and the refinement process has to be defined. During the optimization the parameters are altered in the preselected boundaries by making use of a random number generator [43]. As objective function the error, calculated according to the following equation is used:

$$
error = \frac{100}{2 \cdot p} \sum_{j=1}^{p} \left\{ |i_m(t) - i_s(t)| + \frac{\frac{1}{k}\sum_{i=1}^{k} |T_{i,m} - T_{i,s}|}{T_\infty - T_0} \right\} \quad [\%] \tag{8}
$$

If the smallest predefined variations do not yield any further reduction of the error, the optimum is reached. The first term in Eq. (8) represents the macroscopic mixing behaviour in the tank, while the second part focuses atten-

tion on the micromixing recorded at the sensor locations. The presented error calculation leads to a combination of the parameters balanced between both phenomena.

2.4.4 Surface regression

The surface regression for the adjustable model parameters related to stirrer and aeration Froude-number (in 3D-plots) is calculated by utilizing the PC-Program "GRAFTOOL" (by 3-D Visions Corporation) based on a Maclaurin power series of differing order of the form given by the following equation:

$$\begin{aligned} z(Fr_S, Fr_A) = a_{00} &+ a_{01}Fr_A &+ \cdots + a_{0Y}Fr_A^Y \\ &+ a_{10}Fr_S + a_{11}Fr_SFr_A &+ \cdots + a_{1Y}Fr_SFr_A^Y \\ &\vdots \\ &+ a_{X0}Fr_S^X + a_{X1}Fr_S^XFr_A &+ \cdots + a_{XY}Fr_S^XFr_A^Y \end{aligned} \quad (9)$$

The total number of coefficients computed is the product $(X + 1)(Y + 1)$.

2.5 Verification of the chosen methods

Tests with conventional pulse application to the surface of the liquid were undertaken. Optimization of the model parameters is carried out only for the experiment with central pulse injection (i.e. in $V_{C4,N}$ in case of the STR-3 bioreactor).

In the next step the location of the pulse input in the model is changed to the top (STR-3: in $V_{C1,N}$) while all adjustable model parameters are kept constant. The resulting calculated response functions are compared to the experimental curves resulting from a top pulse dosage.

A sensitivity analysis [11, 20, 27] for all adjustable model parameters in this optimum was undertaken. Each adjustable parameter is altered for $\pm$ 5, 10, ... 25%, except the number of tanks-in-series (N), which is changed by a step of one, since it has to be an integer.

3 Results and discussion

3.1 Verification of the physical mixing model

Basically the utilized mixing models consist of micromixed compartments around the Rushton turbine, i.e. a volume with high turbulent intensity, and macromixed regions characterized by lower turbulence and therefore less backmixing. There are two reasons for the application of these models: Firstly it shall be possible to combine these mixing models with kinetic equations for process control purposes. Secondly the general structure provides the ability to build models for the most common bioreactors, i.e. stirred tank, air-lift [20], bubble-column [20], deep-jet [27, 28], in order to be able to choose the best bioreactor for the particular fermentation. In the model the micromixed compartment is represented by one ideally mixed volume (V_M), while the macromixed circulation loops are simulated through cascades of identical ideally mixed tanks. The size of the ideally mixed volume (V_M) is not only dependent on the amount of introduced energy but also on the aeration rate [46].

In case of the STR-3 bioreactor (3 Rushton turbines) two modifications of the main model were tested:
The first modification had the design proposed by Singh et al. [12]. This model proved to be inadequate for a close description of the hydrodynamic behaviour of the three stage stirred bioreactor, since the response to the tracer appeared immediately in all well mixed compartments because of the direct connections between them. The measurements show a delay in the transit times indicating that the impulse has to pass first through the circulation paths. A direct connection leads to wrong predictions of the exchange flow rates and therefore this approach is too simple.

The attempt to incorporate the gas holdup did not lead to a significant improvement of the physical model, though one more adjustable parameter should give a better fit. The approach tested was not capable to predict the size of the measured gas holdup.

The quality of agreement between measured and simulated response curves is the main criterion for the applicability of the presented physical model. Several steps are involved in order to obtain the parameters of the physical model, each of them has to be verified separately.

The test of the numerical integration method (Runge-Kutta-Fehlberg-algorithm) is demonstrated in Fig. 3 for the STR-1 model with the parameters $N = 2$, $V_M/V_{tot} = 0.2$, $V_{tot} = 1.2\ m^3$, $t_{c,RAD} = 12s$. In this figure the integration results achieved by an exact solution with the Laplace-transformation are compared to the one gained with the Runge-Kutta-Fehlberg-method. The excellent conformity shows the adequacy of the numerical method.

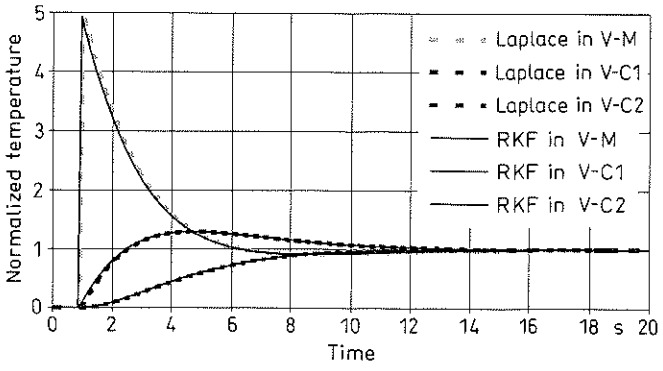

Fig. 3. Comparison of integration results achieved by numerical RKF-method to the ones gained by analytical Laplace solution

The adjustable parameters are optimized by use of a modified Monte-Carlo method. This method is rather slow, but insensitive to large gradients in the objective function as well as to bad initial guesses. Usually 300 integration runs were necessary to reach the optimum with a relative accuracy of 0.001, related on boundaries between 0 and 1. The other tested algorithms, Gauss-Newton-method, collocation-method and Hybrid-method failed, either due to problems solving the Hessenberg-matrix or because of noise in the signals of the sensors.

One of the best methods to test the mixing-model and the experimental setup is an alteration of the pulse input location while all other experimental conditions are fixed, since the real flow pattern should not be influenced by this change. The chosen models as well as the mathematical solutions were tested by means of two different pulse input locations in the STR-3 setup, because in this geometry an alteration in the pulse input location effects the response curves stronger than in the STR-1 tank. The results of these investigations are illustrated in Fig. 4 for the pulse injection in the center of the tank, i.e. close to the bottom side of the middle stirrer (model: in $V_{C4,N}$), and in Fig. 5 for the conventional pulse application to the surface (model: in $V_{C1,N}$). The related model-parameters as well as the experimental conditions are given in the captions.

The model parameters are optimized only in case of Fig. 4. The fit of the model is in the range of the turbulent temperature fluctuations for the sensors in the stirred

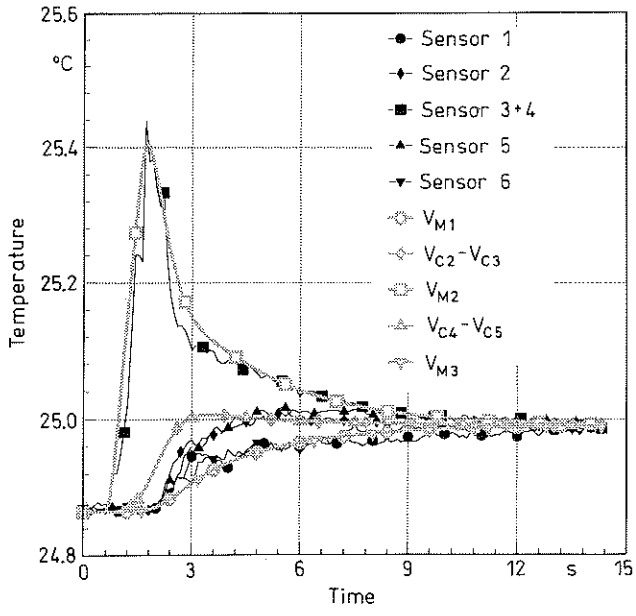

Fig. 4. Measured and simulated response functions for the STR-3 for a central pulse injection. Experimental conditions: $n = 150$ rpm, $F_G = 100$ m^3/h Model parameters: $V_M/V_{tot} = 0.21$, $t_{c,RAD} = 2.05$ s, $t_{c,AX} = 9.15$ s, $N = 3$

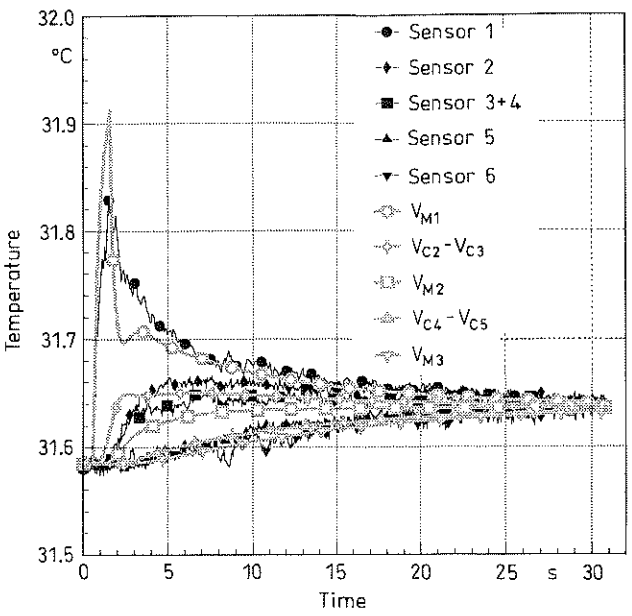

Fig. 5. Measured and simulated response functions for the STR-3, pulse poured onto the surface. Experimental conditions and model parameters are identical to those given for Fig. 4

volumes (V_{M1}, V_{M2}, V_{M3}) . Significant deviations are observed only for the reponse functions in the transient regions (V_{C2}, V_{C5}) in the first part of the experiment, i.e. between 1.5s and 4.5s. Basically the simulated curves fit the measured data correctly.

Looking at Fig. 5 with identical experimental conditions, except for the pulse input location, and identical adjustable parameters, the following conclussion can be drawn:

a) The model fits within the turbulent fluctuations; however, this perfect agreement is achieved mainly in the time period after 12s.
b) The transit time (τ_i) of the flow at the sensor locations are simulated correctly for all sensors, small deviations can be observed only in case of the sensors positioned in V_{M2} and V_{C3}.
c) The peak in the top stirred compartment V_{M1} is predicted quite good.

It is concluded that this model predicts the flow pattern correctly with respect to time constants of all sensors as well as to the mixing time which is about 2.5 times longer for a top-pulse application. Also the maxima at the beginning of the experiments are predicted correctly.

3.2 Optimization of the parameters of the models

A sensitivity analysis of the model is a useful tool to investigate the influence of the different parameters on the objective function, i.e. relative error. The results of the

sensitivity analysis for the STR-3 model are presented in Fig. 6. The more complex STR-3 mixing model was chosen for this demonstration. An analysis of the STR-1 model leads to similar relations, the results are not shown.

The sensitivity analysis indicates that a reduction of the number of tanks (N) in the cascades has the strongest influence on the relative error, mainly due to the large relative variations; since the optimized value for N is 3, a step of $\pm$ 1 already equals a relative change of 33,3%. An increase in N does not lead to alterations of the same magnitude. The second strongest effect on the relative error results from the radial circulation time. The slightest influence appears in case of the relation ideally mixed stirrer volume to total volume V_M/V_{tot}.

For all experiments listed in Table 2 the parameter-estimation procedure was carried out. Figs. 7–9 present the optimized model parameters (V_M/V_{tot}, $t_{c,RAD}$, N) and the regressed surfaces for the bioreactor equipped with one Rushton turbine (STR-1) as a function of two main experimental parameters, i.e. stirrer Froude number Fr_S and aeration Froude number Fr_A, thus including 30 optimized model parameter combinations. The relative error calculated according to Eq. (8) is illustrated in Fig. 10, the data points are fitted by a gridded surface.

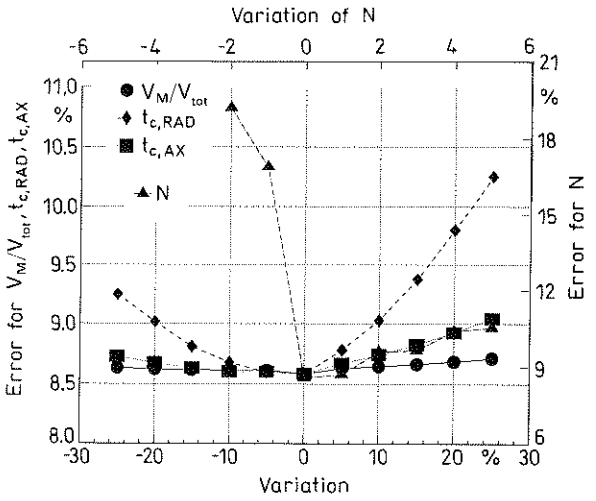

Fig. 6. Parameter sensitivity analysis in the optimum for the STR-3 model. Experimental conditions and model parameters are identical to those given for Fig. 4

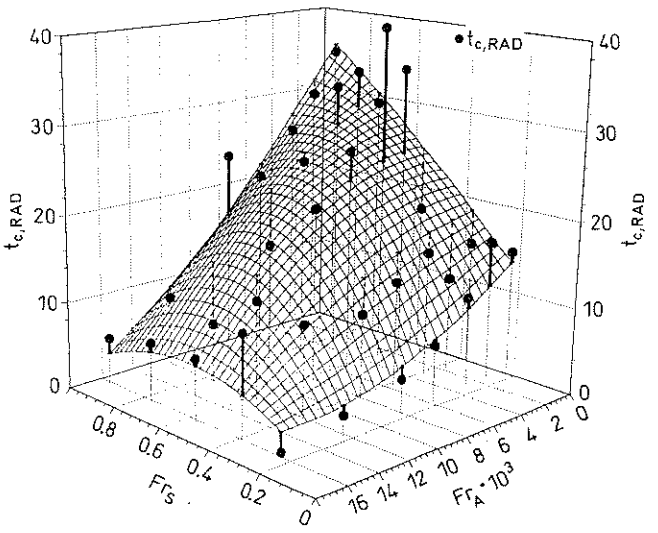

Fig. 8. Dependence of $t_{c,RAD}$ on Froude numbers for stirring and aeration in case of STR-1

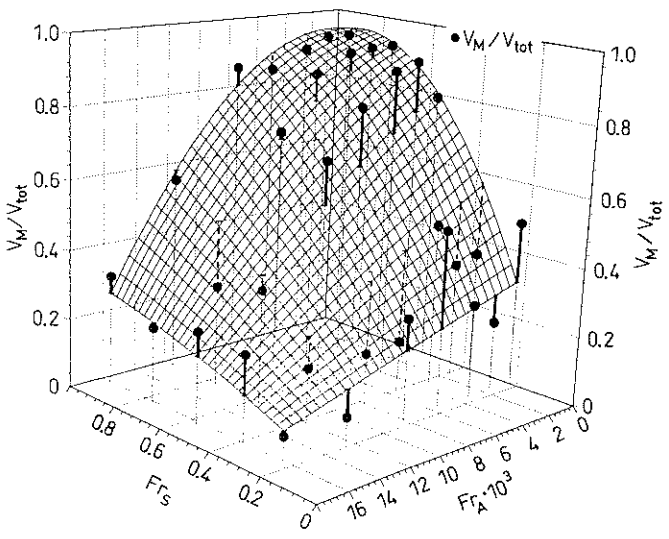

Fig. 7. Dependence of V_M/V_{tot} on Froude numbers for stirring and aeration in case of STR-1

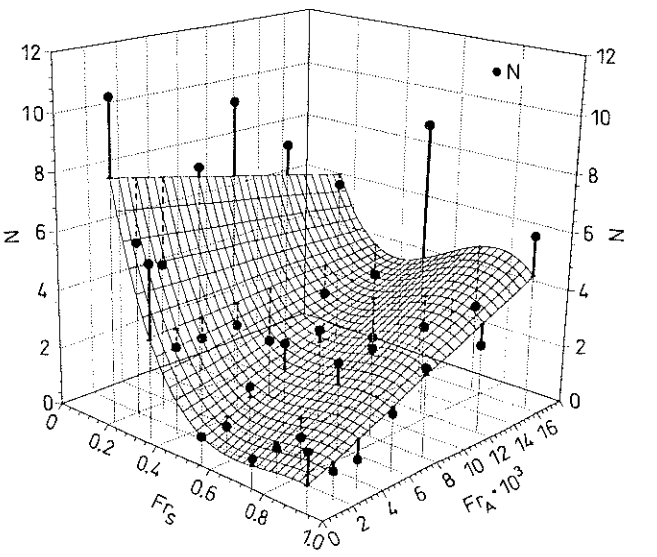

Fig. 9. Dependence of N on Froude numbers for stirring and aeration in case of STR-1

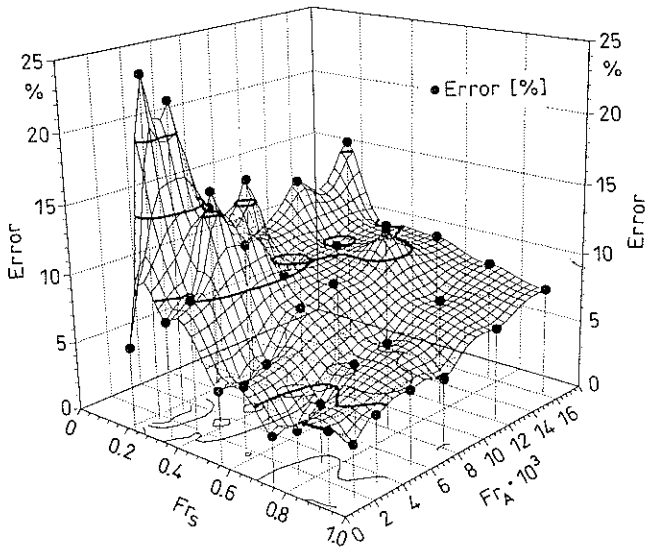

Fig. 10. Dependence of relative error on Froude numbers for stirring and aeration in case of STR-1

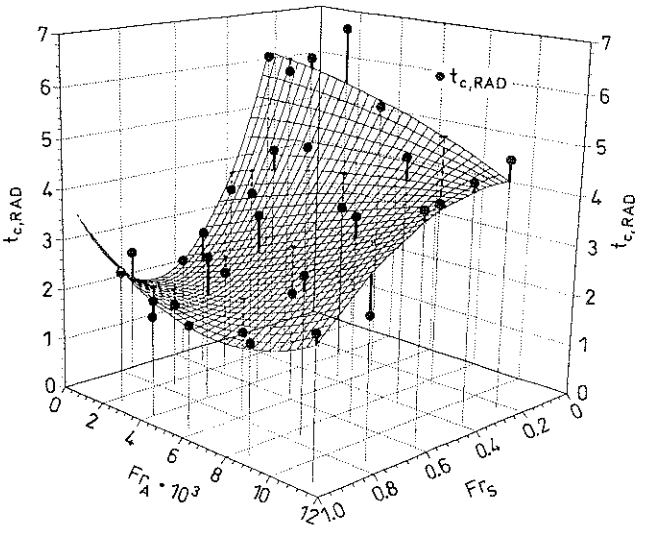

Fig. 12. $t_{c,RAD}$ as function of Froude numbers for stirring and aeration in STR-3 configuration

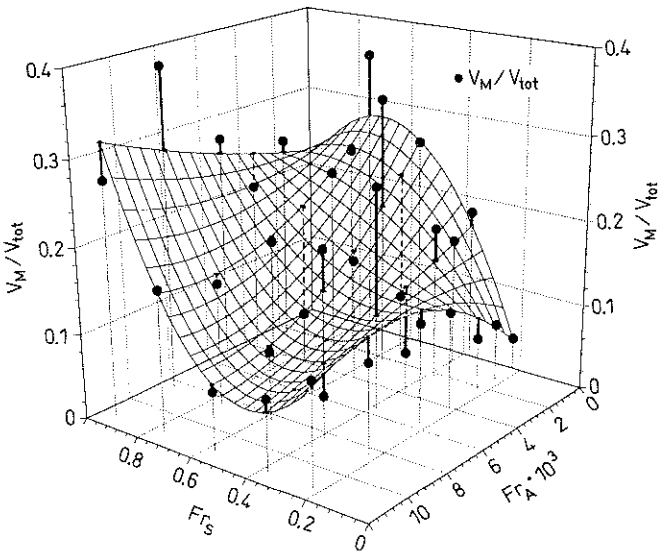

Fig. 11. V_M/V_{tot} as function of Froude numbers for stirring and aeration in STR-3 configuration

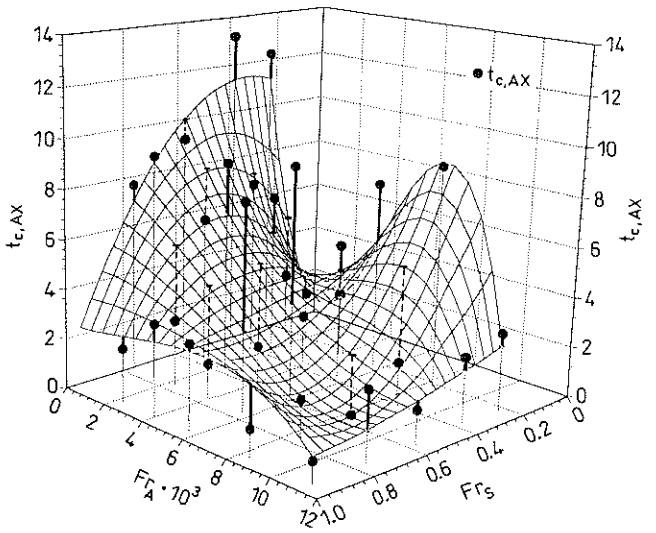

Fig. 13. $t_{c,AX}$ as function of Froude numbers for stirring and aeration in STR-3 configuration

The optimized adjustable model variables, V_M/V_{tot}, $t_{c,RAD}$, $t_{c,AX}$, N, and the regressed surfaces for the bioreactor equipped with three Rushton turbines (STR-3) are presented in Figs. 11–14 as a function of stirrer Froude number Fr_s and aeration Froude number Fr_A. The relative error calculated according to Eq. (8) is illustrated in Fig. 15, the data points are fitted by a gridded surface.

The coefficients for the surfaces plotted in Figs. 7–9 for the STR-1 bioreactor as well as for the Figs. 11–14 in case of the STR-3 tank are given in Table 3 together with the mean deviations of all points related to this surface.

The size of the ideally mixed volume V_M given in Figs. 7 and 11, is strongly dependent on the stirrer Froude number for both configurations. This is in good agreement with results of other investigations [22, 30–37]. An increase in stirrer speed leads to higher power input and consequently to more turbulence in the stirrer region, in fact to a larger micromixed volume. Differences between both setups occur in three aspects.

a) While the aeration rate reduces the size of the ideally mixed volume not significantly in case of STR-3 a strong influence is observed in the STR-1 fermentor.

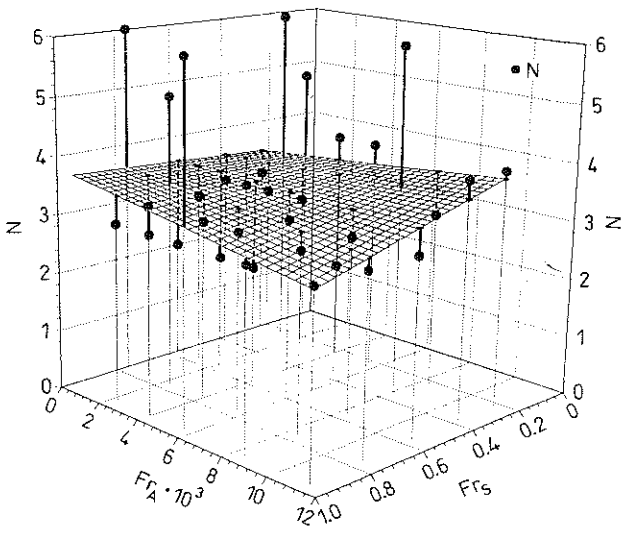

Fig. 14. N as function of Froude numbers for stirring and aeration in STR-3 configuration

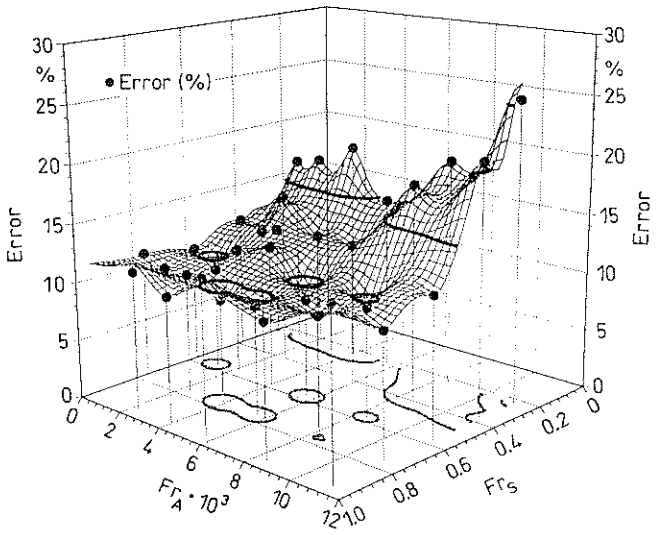

Fig. 15. Relative error as function of Froude numbers for stirring and aeration in STR-3 configuration

This finding indicates that liquid volume is replaced by gas at the stirrer above the gas sparger; this phenomenon is known as forming of gas cavities behind the stirrer blades and in case of high aeration rates as flooding of the stirrer [33, 44, 45]. Since in the STR-3 bioreactor three stirrers are present this influence is diminished [45].

b) The values of the relative size cover the whole range in case of the STR-1 tank, i.e. $0 < V_M/V_{tot} < 1$, while in the STR-3 vessel this relation does not exceed 0.4. This may be interpreted as follows: The circulation paths in the STR-3 need a certain minimum amount of space and

Table 3. Regression coefficients for the fitted surfaces and the mean relative deviation of all points in relation to the surface

Tank	Parameter	Surface regression coefficients acc. to Eq. (9)																		Deviation (%)
		a_{00}	a_{01}	a_{02}	a_{03}	a_{10}	a_{20}	a_{30}	a_{11}	a_{12}	a_{13}	a_{21}	a_{22}	a_{23}	a_{31}	a_{32}	a_{33}	
STR-1	V_M/V_{tot}	−0.219	0.022	−0.001	0	2.643	−1.488	0	−0.203	0.004	0	0.199	−0.007	0	0	0	0	26
	$t_{c,RAD}$	5.261	−4.342	0.240	0	37.20	−5.454	0	16.52	−1.059	0	−15.46	0.891	0	0	0	0	30
	N	22.48	−0.367	0	0	−83.74	105.9	−43.81	1.031	0	0	0.431	0	0	−0.899	0	0	31
STR-3	V_M/V_{tot}	−0.246	0.115	−0.006	0	1.472	−1.029	0	−0.473	0.023	0	0.375	−0.017	0	0	0	0	23
	$t_{c,RAD}$	11.80	−0.611	−0.006	0	−29.86	22.18	0	3.131	−0.023	0	−3.104	0.066	0	0	0	0	14
	$t_{c,AX}$	8.898	−11.89	3.081	−0.184	15.44	−23.60	0	25.10	−8.006	0.500	−13.15	5.053	−0.328	0	0	0	41
	N	3.381	0.071	0	0	0.268	0	0	−0.140	0	0	0	0	0	0	0	0	25

prevent the ideally mixed volume to expand, while in the STR-1 V_M is not limited, but relations larger than $V_M/V_{tot} > 0.8$ are unrealistic and indicate the presence of "dead" volume. This becomes clear by looking at Figs. 7 and 8. Large micromixed volumes correlate with long circulation times.

c) Concerning the radial circulation time $t_{c,RAD}$ (Figs. 8, 12) it can be concluded that this parameter is strictly related to the micromixed volume V_M in case of STR-1 (Fig. 8) and consequently is a "real" model parameter, not related for example to the pumping capacity of the turbine. The physical flow is better matched in case of STR-3 (Fig. 12). The radial circulation time calculated after Eq. (4) drops with increasing stirrer Froude number and depends only in the range of small stirrer Froude values on the aeration Froude number. Generally the radial circulation times in the STR-1 (4–35 s) configuration are longer than in the STR-3 (1.8–7 s).

The axial circulation time $t_{c,AX}$ (Fig. 13), defined by Eq. (5), is less influenced by the stirrer Froude number, but is strongly dependent on the aeration Froude number. The value of the axial circulation time is of the same order of magnitude than that of the radial circulation time. In other words the axial exchange flow rate (see Eq. (5)) is about three times larger than the radial exchange flow at each turbine.

The backmixing parameter N, representing the number of ideally mixed compartments in the recirculation loop, is slightly dependent on stirrer Froude number in case of STR-1 (Fig. 9), while this parameter is fairly constant in the range between 3 to 4 for all experiments in the STR-3 bioreactor (Fig. 14). This is close to the value predicted by Van de Vusse [2] who specified N = 4, but attention must be focused on the fact that for all experiments mentioned in this work a mixture of glycerol with water was used, a different medium might lead to different values.

From Figs. 10 and 15 it is obvious that the proposed models fit better for a stirrer regime, as the error declines with increasing Fr_s and decreasing Fr_A. This is in fact an expected property, since the model was established for stirred tank bioreactors. In these figures the contour lines indicate constant relative error in steps of 5%.

Further work should clarify the significance of this approach for scale-up predictions.

4 Conclusion

On basis of the inhomogeneity-curve the optimization of the adjustable parameters of mixing models using the tank-in-series concept was successfully accomplished with the application of the Monte-Carlo-routine.

Outstanding results are the following:
A suitable test for mixing models is a variations in the pulse input location. The model should be able to simulate both cases (see Figs. 4 and 5).
For the STR-1 stirred tank the following conclusions should be observed;

a) It seems adviseable to include a "dead" zone connected to the cascade in the mixing model, since the situation is more complex. From Figs. 7 and 8 it can be seen that increased V_M is correlated with increased $t_{c,RAD}$ at high values of Fr_S. This situation can only occur at low levels of Fr_A, thus indicating that high aeration destroys the "dead" zone.

b) The number of ideally mixed tanks in the cascade is strongly related to Fr_S and lies in the magnitude of 1–7 (Fig. 9).
For the STR-3 stirred tank the following conclusion should be observed;

a) The ratio of the well mixed compartment related on the total liquid volume is mainly a function of stirrer speed and lies between 0.1 and 0.3 (Fig. 11).

b) The radial circulation time is more or less independent from Fr_A and is in the range of 1.8–7.0 s (Fig. 12).

c) The axial circulation time in the range of 2–12 s mainly depends on Fr_A (Fig. 13).

d) The number of ideally mixed tanks in the cascade is nearly constant at $N = 4$ (Fig. 14).

e) The physical model matches the flow properties correctly, if the axial exchange flow is assigned to the cascades.

The relative error defined according to Eq. (8) is in the range of 5–20% for all optimized experiments, which is a satisfying deviation for flow models (Figs. 10 and 15).

Acknowledgement

This work was kindly supported by the Austrian "Ministerium für Wissenschaft und Forschung" within the project B12 "Bioreaktoren und Bioprozesse".

References

1. Dankwerts, P. V.: Continuous flow systems. Chem. Eng. Sci., 2 (1953) 1–13
2. Van de Vusse, J. G.: A new model for the stirred tank reactor. Chem. Eng. Sci., 17 (1962) 507–521
3. Sheppard, C. W.: Basic principles of the tracer method. New York: John Wiley and Sons 1962
4. Aris, R.: Compartmental analysis and the theory of residence time distribution. in: Intracellular Transport. New York: Academic Press 1966
5. Resugno, A.; Segre, G.: Drug and tracer kinetics. London: Blaisdell Pub. Co. 1966
6. Sinclair, C. G.; Brown, D. E.: Effect of incomplete mixing on the analysis of the static behaviour of continuous cultures. Biotechnol. Bioeng. 12 (1970) 1001–1017
7. Wen, C. Y.; Fan, L. T.: Models for flow systems and chemical reactors. New York: Marcel Dekker Inc. 1975

8. Levenspiel, O.: Chemical Reaction Engineering. New York: John Wiley and Sons 1972
9. Khang, S. J.; Levenspiel, O.: New scale up and design method for stirrer agitated batch mixing vessels. Chem. Eng. Sci. 31 (1976) 569–577
10. Levenspiel, O.: Chemical Reactor Omnibook. Corvallis OR: OSU Book Stores Inc. 1979
11. Oosterhuis, N. M. G.; Kossen, N. W. F.: Modelling and scaling-up of bioreactors. in: Brauer, H.: Fundamentals of biochemical engineering, Biotechnology (Vol. 2), Weinheim, Deerfield Beach FL VCH (1985) 571–605
12. Singh, V.; Hensler, W.; Fuchs R.: Online determination of mixing parameters in fermentors using pH transient. in: Bioreactor Fluid Dynamics, Paper 18, Cambridge (1986) 231–256
13. Singh, V.; Fuchs, R.; Constantinides, A.: A new method for fermentor scale-up incorporating both mixing and mass transfer effects - I. Theoretical basis. in: Ho, C. S.; Oldshue, J. Y.; (Eds.): Biotechnology Processes, Scale-up and Mixing. New York: AIChE Publ. (1987) 200–214
14. Singh, V.; Fuchs, R.; Constantinides, A.: Use of mass transfer and mixing correlation for the modelling of oxygen transfer in stirred tank fermentors. in: Bioreactor Fluid Dynamics, Proc. 2nd Int. Conf. Cranfield, UK (1988) 95–115
15. Bader, F. G.: Modelling mass transfer and agitator performance in multiturbine fermentors. Biotechnol. Bioeng. 30 (1987) 37–51
16. Bader, F. G.: Improvements in multiturbine mass transfer models. in: Ho C. S., Oldshue, J. Y., (Eds.) : Biotechnology Processes, Scale-up and Mixing. New York: AIChE Publ. (1987) 96–106
17. Bajpai, R. K.; Sohn, P. U.: Stage models for mixing in stirred bioreactors. in: Ho C. S., Oldshue, J. Y., (Eds.) : Biotechnology Processes, Scale-up and Mixing. New York, AIChE Publ. (1987) 13–21
18. Moser, A.: Bioprocess Technology. New York, Wien: Springer Verlag (1988)
19. Heinzle, E.; Kaufmann, T.; Griot, M.: Modelling of kinetics, mass transfer and mixing. in: Fish, N. M.; Fox, R. I.; Thornhill, N. F. (Eds.) : Computer application in fermentation technology. New York, London: Elsevier Applied Science (1989) 105–109
20. Jury, W.: Mixing in bioreactors. Ph.D. Thesis, Institute for Biotechnology, Graz University of Technology 1989
21. Ragot, F.; Reuss, M.: A multi-phase compartment model for stirred bioreactors incorporating mass transfer and mixing. 2nd Int. Symp. on Biochemical engineering, Stuttgart. 1990
22. Henzler, H. J.; Obernosterer, G.: Effect of mixing behaviour on gas-liquid mass transfer in highly viscous stirred non-Newtonian liquids. Chem. Eng. Technol. 14 (1991) 1–10
23. Reuss, M.; Bajpai, R.: Stirred tank models. in: Rehm, H. J., Reed G., Pühler, A., Stadler, P. (Eds.) : Biotechnology. Schügerl K. (Volume Ed.) : Measuring, modelling and control. Vol. 4 Weinheim, New York, Basel, Cambridge: VCH Verlagsgesellschaft 1991
24. Dankwerts, P. V.: The effect of incomplete mixing on homogeneous reactions. Chem. Eng. Sci., 8 (1958) 93–102
25. Schneider, G.; Purgstaller, A.; Somitsch, H.; Moser, A.: Approach to mixing in bioreactors – experimental verification, methodology and model bioreactor. in: Chmiel, H. et al. (Eds.): Biochemical Engineering. Stuttgart, New York: G. Fischer Verlag (1987) 428–430
26. Mayr, B.; Horvat, P.; Moser, A.: Engineering approach to mixing quantification in bioreactors. Biopr. Eng. 8 (1992) 137–143
27. Moser, A.; Mayr, B.; Jury, W.; Steiner, W.; Horvat, P.: Mathematical models for mixing in deep jet bioreactor: Analysis. Biopr. Eng. 7 (1991) 171–176
28. Moser, A.; Mayr, B.; Jury, W.; Steiner, W.; Horvat, P.: Mathematical models for mixing in deep jet bioreactor: Calculation of parameters. Biopr. Eng. 7 (1991) 177–182
29. Jury, W.; Schneider, G.; Moser, A.: Modelling approach to industrial bioreactors. in: 6th European Conference on Mixing, Pavia, Italy, organized by AIDIC (1988) 451–456
30. Cutter, L. A.: Flow and turbulence in a stirred tank. AIChE J. 12 (1966) 35–45
31. Günkel, A. A.; Weber, M. E.: Flow phenomena in stirred tanks. AIChE J. 21 (1975) 931–949
32. Nagata, S.: Mixing principles and applications. New York, John Wiley & Sons 1975
33. Brauer, H.: Power consumption in aerated stirred tank reactor systems. Adv. Biochem. Eng., 13 (1979) 87–119
34. Moeckel, H. O.: Die Verteilung der örtlichen Energiedissipation in einem Rührwerk. Chem. Tech. 32 (1980) 127–129
35. Okamoto, Y.; Nishikawa, M.; Hashimoto, K.: Energy dissipation rate distribution in mixing vessels and its effects on liquid-liquid dispersion and solid-liquid mass transfer. Chem. Eng. 21 (1981) 88–94
36. Placek, I.; Tavlarides, L. L.; Smith, G. W.; Fort I.: Turbulent flow in stirred tanks. Part II: A two scale model of turbulence. AIChE J. 32 (1986) 1771–1786
37. Laufhütte, H. D.; Mersmann, A.: Die lokale Energiedissipation im turbulent gerührten Fluid und ihre Bedeutung für die verfahrenstechnische Auslegung von Rührwerken. CIT, 57 (1986) 1104–1105
38. Fehlberg, E.: Klassische Runge-Kutta Formeln vierter und niedrigerer Ordnung mit Schrittweiten-Kontrolle und ihre Anwendung auf Wärmeleitungsprobleme. Computing, 6 (1970) 61–71
39. Burden, R. L.; Faires, J. D.: Numerical Analysis. Boston: PWS Publishers 1985
40. Dennis, J. E.: Non-linear least squares and equations. in: Jacobs (Ed): The state of art in numerical analysis. Proceedings of the conference on the state of art in numerical analysis London, New York, San Francisco: Academic Press 1977
41. Walsh, G. R.: Methods of optimization. London, New York, Sydney, Toronto: John Wiley and Sons 1975
42. Späth, H.: Algorithmen für multivariante Ausgleichsmodelle. München, Wien: R. Oldenbourg Verlag 1974
43. Knuth, D. E.: Seminumerical Algorithms. in: The art of computer programming, Addison Wesley Publishing Company 1982
44. Manning, S. A.; Jameson, G. L.: A study of ventilated gas cavities on disc-turbine blades. in: 7th European Conference on Mixing proceedings volume I, Brugge: Royal Flemish Society of Engineers (1991) 225–231
45. Smith, J. M.: Simple performance correlations for agitated vessels. in: 7th European Conference on Mixing, Proceedings Volume I, Brugge: Royal Flemish Society of Engineers (1991) 233–242
46. Patterson, G. K.: Measurements and modelling of flow in gas sparged, agitated vessels. in: 7th European Conference on Mixing. Proceedings Volume I, Brugge: Royal Flemish Society of Engineers (1991) 209–215

Received May 6, 1992

Mayr B.
Moser A. (corresponding author)
Institute for Biotechnology
Petersgasse 12, 8010 Graz,
Austria

Horvat P.
Faculty of Food Technology and Biotechnology
University of Zagreb
Pierottijeva 6, 41000 Zagreb,
Croatia

Nagy E.
Research Institute for Technical Chemistry of Hungarian Academy of Sciences P.O. Box 125, 8201 Veszprém,
Hungary